MEIG1 is essential for spermiogenesis in mice

Zhibing Zhang[a,b,1], Xuening Shen[a], David R. Gude[a,b], Bonney M. Wilkinson[c], Monica J. Justice[c], Charles J. Flickinger[d], John C. Herr[d], Edward M. Eddy[e], and Jerome F. Strauss III[a,b]

Departments of [a]Obstetrics and Gynecology and [b]Biochemistry, Virginia Commonwealth University, Richmond, VA 23298; [c]Department of Molecular and Human Genetics, Baylor College of Medicine, One Baylor Plaza, Houston, TX 77030; [d]Department of Cell Biology, Center for Research in Contraceptive and Reproductive Health, University of Virginia, 1300 Jefferson Park Avenue, Charlottesville, VA 22908; and [e]Laboratories of Reproductive and Developmental Toxicology, National Institute of Environmental Health Sciences, National Institutes of Health, Research Triangle Park, NC 27709

Edited by Abraham Kierszenbaum, City University of New York, and accepted by the Editorial Board August 6, 2009 (received for review June 9, 2009)

Spermatogenesis can be divided into three stages: spermatogonial mitosis, meiosis of spermatocytes, and spermiogenesis. During spermiogenesis, spermatids undergo dramatic morphological changes including formation of a flagellum and chromosomal packaging and condensation of the nucleus into the sperm head. The genes regulating the latter processes are largely unknown. We previously discovered that a bi-functional gene, *Spag16*, is essential for spermatogenesis. SPAG16S, the 35 kDa, testis-specific isoform derived from the *Spag16* gene, was found to bind to meiosis expressed gene 1 product (MEIG1), a protein originally thought to play a role in meiosis. We inactivated the *Meig1* gene and, unexpectedly, found that *Meig1* mutant male mice had no obvious defect in meiosis, but were sterile as a result of impaired spermatogenesis at the stage of elongation and condensation. Transmission electron microscopy revealed that the manchette, a microtubular organelle essential for sperm head and flagellar formation was disrupted in spermatids of MEIG1-deficient mice. We also found that MEIG1 associates with the Parkin co-regulated gene (PACRG) protein, and that testicular PACRG protein is reduced in MEIG1-deficient mice. PACRG is thought to play a key role in assembly of the axonemes/flagella and the reproductive phenotype of *Pacrg*-deficient mice mirrors that of the *Meig1* mutant mice. Our findings reveal a critical role for the MEIG1/PARCG partnership in manchette structure and function and the control of spermiogenesis.

Spermatogenesis can be divided into three stages: spermatogonial mitosis, meiosis of spermatocytes, and spermiogenesis, the final step of spermatogenesis. During this stage, the haploid round spermatids differentiate into species-specific shaped spermatozoon, with dramatic morphological changes, including elongation and condensation of the nucleus, and formation of the flagellum (1, 2). Even though some genes have been reported to be indispensable for this process (3, 4), the underlying mechanisms remains largely unknown and need to be elucidated.

Mouse meiosis expressed gene 1 (*Meig1*) was originally identified in a search for mammalian genes potentially involved in meiosis. Two *Meig1* transcripts, 11a2 and 2a2, were identified previously, both containing three exons. The two transcripts share the same ORF and 3′ UTR, but differ in their 5′ UTRs. Each has a unique non-translated exon 1. The 11a2 message was expressed in somatic cells in the testis, including Leydig cells, whereas the predominant 2a2 isoform was reported to be germ cell-specific. The 2a2 transcript begins to accumulate in the testis at day (d)8–9 of postnatal (pn) development, coinciding with the entry of germ cells into meiosis, and is expressed most abundantly at pn d14 and subsequent stages, when spermatocytes enter the pachytene stage. In situ hybridization analysis showed that *Meig1* expression level was low in leptotene cells and increased as the cells progressed through zygotene and pachytene stages. In addition, *Meig1* message was also detected in embryonic ovary after d15 of gestation when the cells entered the pachytene stage of meiosis 1, but not in adult ovary, suggesting that *Meig1* is a meiosis-associated gene (5–9). A recent transcriptional profile study revealed that the *Meig1* message is also present in Sertoli cells in fetal gonads and a Sertoli cell line TTE3 (10, 11). Although the molecular weight is 10 kDa according to its amino acid composition, MEIG1 protein migrates as a 14-kDa band in Western blots because of its basic nature. MEIG1 protein contains multiple consensus sequences for serine and threonine phosphorylation. There is also evidence that MEIG1 protein is phosphorylated and forms a dimer in vivo (8). Furthermore, the phosphorylated dimer enters the nucleus during the first meiotic prophase and binds to meiotic chromatin (9).

The function of MEIG1 remains unknown. Our previous investigation revealed that MEIG1 associates with SPAG16S, a 35-kDa nuclear protein essential for spermatogenesis (12). Recent studies by others also suggested that MEIG1 might be essential for spermatogenesis and related to ciliary function. *Meig1* message is dramatically reduced in heat shock transcription factor 2 (Hsf2) mutant mice, and this may result in impaired spermatogenesis and reduced fertility of *Hsf2* mutant mice (13). A bioinformatic analysis revealed that *Meig1* is most abundantly expressed in tissues rich in ciliated cells, such as, testis, lung, olfactory sensory neurons, and is, therefore, predicted to be important for cilia function (14).

To investigate the function of the *Meig1* gene, we generated a *Meig1*-conditional knockout mouse model, and crossed it to CMV-Cre transgenic mice so that the *Meig1* gene was deleted globally in vivo. Our studies with the globally targeted *Meig1*-knockout mice indicate that homozygous mice are viable, but the males are sterile, producing only a few sperm that are morphologically abnormal. Spermatogenesis is dramatically impaired at the stage of elongation and condensation. These studies indicate that MEIG1 is a key protein in the regulation of spermiogenesis.

Results

To predict potential function of the MEIG1 protein, the mouse MEIG1 protein sequence was analyzed for conserved domains with NCBI conserved domain program (http://www.ncbi.nlm.nih.gov/Structure/cdd/cdd.shtml). No known functional domains were identified. However, the MEIG1 protein sequences were found to be highly conserved among different species (Fig. S1).

To further characterize the *Meig1* gene, 5′ RACE was conducted with a *Meig1* specific reverse primer localized in exon 1. The PCR products were cloned into pCR2.1 TA vector, and 20 inserts were fully sequenced. Three isoforms were identified, *Meig1_v1*, *Meig1_v2*, and *Meig1_v3*. *Meig1_v1* and *Meig1_v2* correspond to 11a2 and 2a2, respectively, *Meig1_v3* is a previously unidentified isoform. This isoform also shares the same coding sequences as *Meig1_v1* and *Meig1_v2*, but it has a unique non-translated exon in front of the first coding exon (Fig. 1*A*). Thus, the three isoforms can be distinguished by their non-translated exons. To further investigate the tissue distribution and expression patterns during the first wave of sper-

Author contributions: Z.Z. designed research; Z.Z., X.S., D.R.G., and B.M.W. performed research; B.M.W. and M.J.J. contributed new reagents/analytic tools; Z.Z., C.J.F., J.C.H., E.M.E., and J.F.S. analyzed data; and Z.Z. wrote the paper.

The authors declare no conflict of interest.

This article is a PNAS Direct Submission. A.K. is a guest editor invited by the Editorial Board.

Freely available online through the PNAS open access option.

[1]To whom correspondence should be addressed. E-mail: zzhang4@vcu.edu.

This article contains supporting information online at www.pnas.org/cgi/content/full/0906414106/DCSupplemental.

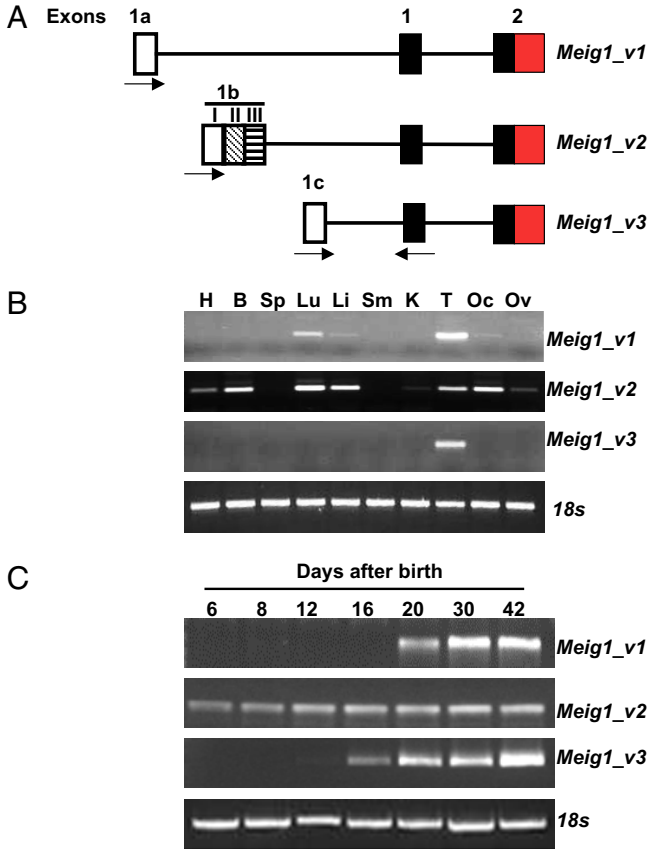

Fig. 1. Expression patterns of the three *Meig1* isoforms. (*A*) Structure of the *Meig1* gene. Solid boxes indicate translated exons (1 and 2), open, notched, and crossed boxes indicate nontranslated exons (1a, 1b, and 1c). The arrows indicate location of RT-PCR primers. The red solid boxes indicate 3′UTR of the *Meig1* transcripts. I, II, III under 1b represent three consecutive sequences in the exon. (*B*) Tissue distribution of the three *Meig1* transcripts. H: heart; B: brain; SP: spleen; Lu: lung; Li: liver; Sm: skeletal muscle; K: kidney; T: testis; Oc: oocyte; Ov: oviduct. (*C*) mRNA expression of the three *Meig1* transcripts during the first wave of spermatogenesis (RT-PCR analysis).

matogenesis, primer sets were designed so that the three isoforms could be amplified separately. The reverse primer is located in exon 1, the forward primers are in individual non-translated exons (Fig. 1*A*, 1a for *Meig1_v1*, 1b for *Meig1_v2*, and 1c for *Meig1_v3*). PCR was performed using cDNAs reversely transcribed from total RNA isolated from different tissues. *Meig1_v1* message, which was reported to be a somatic isoform, was present in several tissues tested, including lung, liver, testis, and oocytes; *Meig1_v2*, which was reported to be germ cell-specific isoform, was present in almost all of the tissues analyzed (Fig. 1*B*). The other isoform we identified, *Meig1_v3* was only expressed in the testis (Fig. 1*B*). Expression patterns of the three isoforms were also investigated during the first wave of spermatogenesis (Fig. 1*C*). *Meig1_v1* message was present from d20 after birth, *Meig1_v2* was present throughout the whole process of spermatogenesis, *Meig1_v3* was detectable from d12 after birth, and the message was abundant in a late stage of spermiogenesis.

The Ensemble Genome Browser shows five distinct *Meig1* transcripts in the mouse: *Meig1*-001, 002, 003, 004, and 005. Sequences of these five transcripts were compared with the three *Meig1* transcripts we identified. *Meig1*-002 is identical to *Meig1-v1*; *Meig1*-001 is identical to *Meig1-v2*, except that it lacks sequence I; and *Meig1*-005 contains an extra sequence (IV) compared to *Meig1*-001. *Meig1*-003 and *Meig1-v3* share the same coding exons and the nontranslated exon 1c, but *Meig1*-003 contains an extra nontranslated exon, sequence III in 1b. *Meig1*-004 contains the same coding sequence as the other *Meig1* transcripts, but a shorter 3′UTR, in addition, its nontranslated exon is located between 1b and 1c (Fig. S2). Specific primers were designed for PCR amplification of *Meig1*-004 and *Meig1*-005. *Meig1*-004 is only present in the testis. Besides being highly expressed in the testis, *Meig1*-005 was present in most of the tissues tested, including brain, lung, and oviduct (Fig. S2*Ba*). During the first wave of spermatogenesis, *Meig1*-004 is detectable from d8 after birth, *Meig1*-005 is expressed as early as d6 after birth, and the message is up-regulated during spermatogenesis (Fig. S2*Bb*).

To investigate the role of the *Meig1* gene in vivo, we generated a *Meig1*-conditional knockout mouse model using the LoxP system. The targeting strategy is shown in Fig. S3*A*. LoxP sites were inserted upstream and downstream of the first coding exon, exon 1. The targeting construct was linearized by *ClaI* digestion at the plasmid/gene insert junction and transfected into the XY ES cells by electroporation. The ES clones were screened by PCR with a forward primer located in the *Neo* cassette of the target construct, and a reverse primer located downstream of the right arm; or a forward primer located upstream of the left arm, and a reverse primer located in the *Neo* cassette (as shown in Fig. S3*A*). Five positive ES cell clones were identified by PCR and were further confirmed by Southern blotting using a probe as shown in Fig. S3*A* corresponding to an upstream region flanking the mutation site. The probe recognized a 10-kb DNA fragment in the wild-type allele and a 7-kb DNA in the targeted allele when DNA was digested by *BamH I* (Fig. S3*B*). ES cells from 2 different clones verified to contain the properly *Meig1*-mutated gene were injected into blastocysts to produce chimeric mice. The chimeric male mice were bred to wild-type female mice to create heterozygous mice without deletion of any genomic sequence (Fig. S3*C*). These heterozygous mice were crossed to FLP recombinase transgenic mice to delete the *Neo* cassette, and the resulting mice (*Meig1*^{flox} mice) were crossed with CMV-Cre transgenic mice expressing Cre recombinase and thus deleting exon 1 of the *Meig1* gene during embryogenesis.

When *Meig1*^{flox} mice were crossed to CMV-Cre transgenic mice, it was found that the mutant allele could be transmitted from both *Meig1* heterozygous males and females, and that homozygous mice could be obtained from interbreeding of the heterozygous male and female mice (Fig. 2*A*). Both male and female null mice were viable and showed no gross abnormalities associated with cilia dysfunction in mice, including failure to thrive, hydrocephalus, *situs inversus*, sinus, and pulmonary infection. Northern blot and RT-PCR analyses revealed that the *Meig1* messages were undetectable in the testis, and all other somatic tissues evaluated (Fig. 2 *B* and *C* and Fig. S2*Bc*). Western blot analysis using testis extracts demonstrated that MEIG1 protein was absent in the *Meig1*-null mice (Fig. 2*D*).

To test fertility of the *Meig1* mutant mice, mature nullizygous mice (>6 weeks of age) were mated with wild-type mice. All of the wild-type (*Meig1*^{flox}), heterozygous and homozygous female mice tested delivered pups with normal litter sizes. Wild-type and heterozygous males were also fertile. However, all nine homozygous mutant male mice tested were sterile through 4 months of breeding (Table 1).

The testis weight of the nullizygous mice euthanized at 6 months of age was comparable to age-matched wild-type mice (Table 1). Light microscopy revealed that in wild-type and heterozygous adult mice, all stages of spermatogenesis were present (Fig. 2*E* and Fig. S4). However, in *Meig1* homozygous mutant mice, microscopy revealed that most spermatids developed only up to steps 12–13, a few to steps 14–15, and beyond that most had been shed (Fig. 2*E* and Fig. S4). Even though spermiogenesis is arrested before complete spermatid elongation, there was no significant differences in the DNA content of cell populations between wild-type and *Meig1* mutant mice as analyzed by flow cytometry using adult mice, indicating no defects in meiosis (Fig. 2*F*). In epididymides from

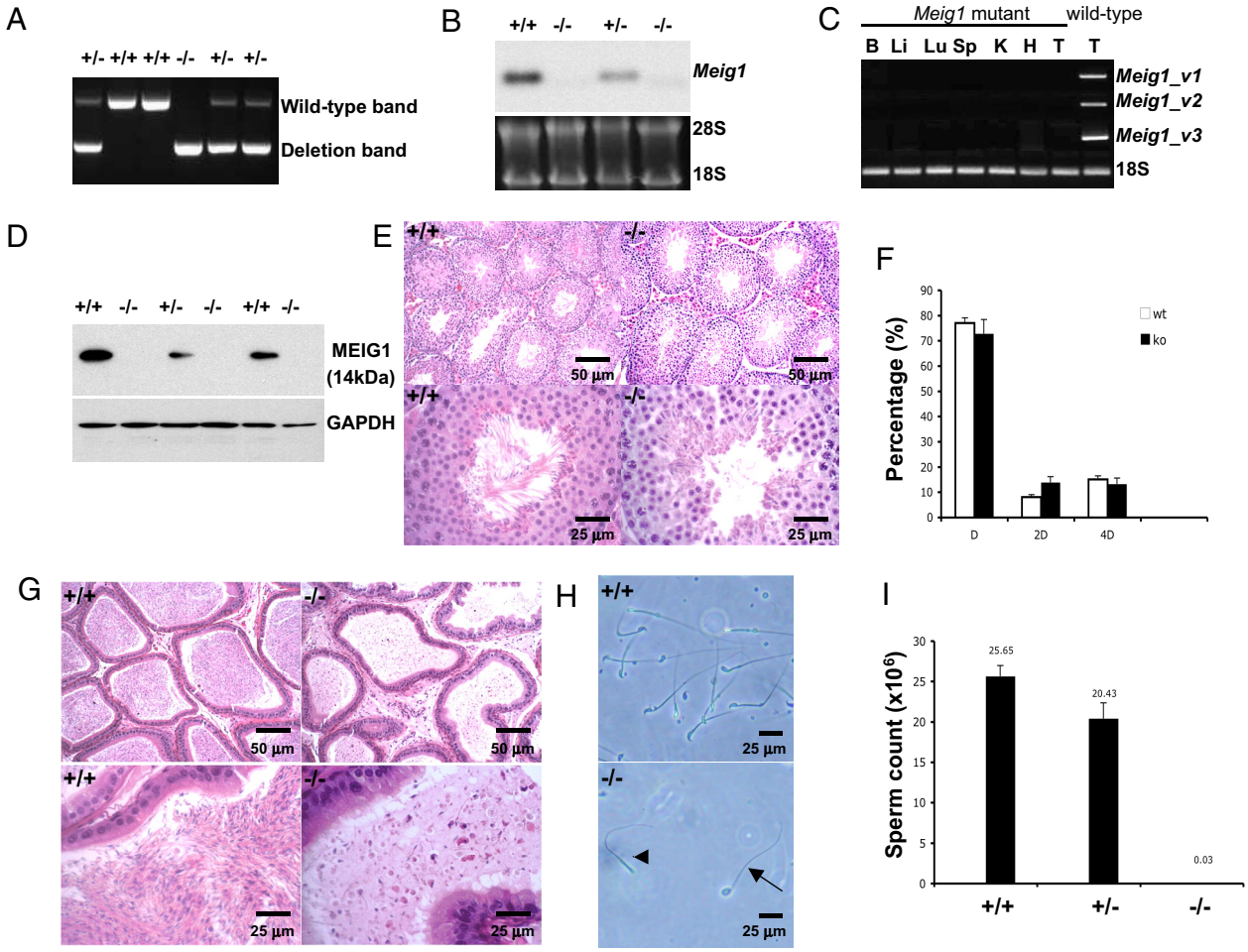

Fig. 2. Phenotype of *Meig1/CMV-Cre* mutant mice. (*A*) Representative PCR results using a primer set (P3 and P4 in Fig. S3*A*, primer sequences in Table S1) showing heterozygous (+/−), wild-type (+/+), and homozygous (−/−) genotypes. (*B*) Northern blot analysis of testicular *Meig1* mRNA expression in wild-type, heterozygous and homozygous mice with *Meig1* full-length cDNA as the probe. (*C*) All of the three *Meig1* transcripts are disrupted in all of the tissues in *Meig1/CMV-Cre* mice as revealed by PCR using isoform specific primers sets. B: brain; Li: liver; Lu: lung; Sp: spleen; K: kidney; H: heart; T: testis. (*D*) Western blot analysis of testicular MEIG1 protein expression in wild-type, heterozygous and homozygous mice. (*E*) Representative testicular H&E staining images from wild-type and *Meig1* homozygous mutant mice. (*F*) Analysis of haploid (D), diploid (2D), and tetraploid cells (4D) cell populations in wild-type and knockout mice by flow cytometry. (*G*) Representative images of epididymides from a wild-type mouse (+/+) and a *Meig1* homozygous mutant mouse (−/−). (*H*) Representative sperm collected in 2 mL PBS from cauda epididymides from a wild-type (+/+) and a *Meig1* homozygous (−/−) mice. The arrow points to a sperm with a round head, the arrow head points to a sperm with a detached head. (*I*) Sperm count of wild-type (+/+), heterozygous (+/−), and homozygous (−/−) mice. $n = 8$ for each group. *: $P < 0.001$.

wild-type adult mice, typical adult sperm concentrations were found (Fig. 2*G*), but epididymides from *Meig1* homozygous mutant mice only contained debris and degenerating sperm, none of which were motile as examined by visual inspection with a light microscope (Fig. 2 *G–I*). Histological evaluation of the lung, brain, heart, kidney and liver revealed normal tissue architecture. Transmission electron microscopy demonstrated that spermatids in wild-type mice undergo the normal developmental process, including flagella formation and chromatin condensation and have a normal manchette structure (Fig. 3 *A–D* and Fig. S5). However, in *Meig1*-deficient mice, there was failure of flagellar formation, disorganization of sperm axonemes, and deformed sperm heads, no obvious or disrupted manchette structures were seen in spermatids (Fig. 3 *E–L* and Fig. S6). We also observed condensed Sertoli cell cytoplasm. A normal "9 + 2" axoneme arrangement was not present in the flagellum of MEIG1-deficient spermatids, and some flagella contained multiple axoneme structures. Interestingly, flagellar components such as microtubules and outer dense fibers could be detected but were not assembled correctly. This is consistent with the normal expression of genes encoding axoneme and fibrous

Table 1. Fertility, fecundity, and testis weight of wild-type and *Meig1* mutant mice

Genotype	Male fertility	Litter size ($n = 8$)	Testis/body weight ($n = 8$, mg/g)	Female fertility	Litter size ($n = 8$)
+/+	8/8	8.6 ± 0.6	8.15 ± 0.41	8/8	9.4 ± 0.5
+/−	8/8	8.4 ± 0.4	8.05 ± 0.35	8/8	9.6 ± 0.4
−/−	9/0	0	7.95 ± 0.41	8/8	10.1 ± 0.6

To test fertility, sexually mature mice were bred to wild-type animals for four months. Litter size was recorded for each mating. Testis weight and body weight were measured from adult mice.

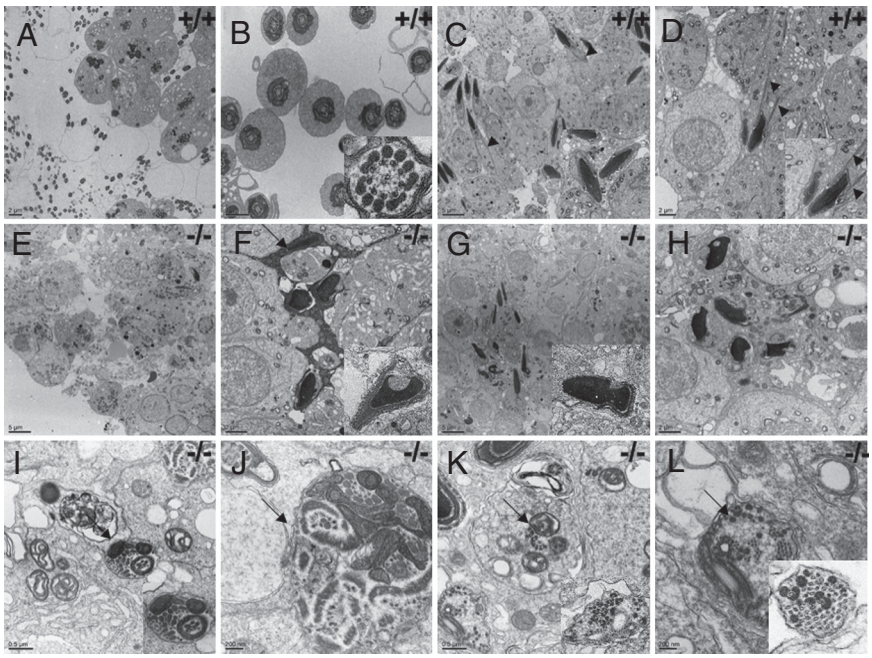

Fig. 3. Testicular ultrastructure in adult wild-type and *Meig1* mutant mice. Representative transmission electronic microscopy images from an adult wild-type mouse (*A–D*) and a *Meig1* homozygous mutant mouse (*E–L*). *A* and *B* show normal spermatogenesis and axoneme structure in wild-type testes, *C* and *D* shows normal condensing spermatids heads and manchette structure (arrow heads) in wild-type testes. *E* shows failure of spermatogenesis as evaluated by absence of sperm in the lumen of seminiferous tubule. *F* represents highly condensed Sertoli cell cytoplasm (arrow). *G* and *H* represent some condensing spermatids that lack manchette structure as seen in the wild-type testes (*C* and *D*). Inserts in *F* and *G* represent two deformed sperm heads. *I–L* and inserts show disorganized flagella. Note that the flagella components, such as microtubules and outer dense fibers seem to be made normally, but are not assembled correctly into flagella. Some flagella contain multiple axonemal structure (*J*). Arrows point to disorganized flagella.

sheath proteins in the MEIG1-deficient mice (Fig. S7) and the observation that TNP2 failed to translocate into nuclei of spermatids in *Meig1*-deficient mice (Fig. S8).

To explore possible mechanisms of MEIG1 action, we carried out a yeast two-hybrid screen to identify interacting partners. Among the 70 positive clones sequenced, 18 represented PACRG. This interaction was confirmed by co-immunoprecipitation from lysates of MEIG1 and PACRG co-transfected COS-1 cells (Fig. 4 *A* and *B*), and testicular extracts (Fig. S9). Interestingly, testicular PACRG protein, but not mRNA expression, was reduced in *Meig1* mutant mice. However, in *quaking* mutant mice in which the *Pacrg* gene is deleted, testicular MEIG1 protein was unchanged (Fig. 4 *C–E*).

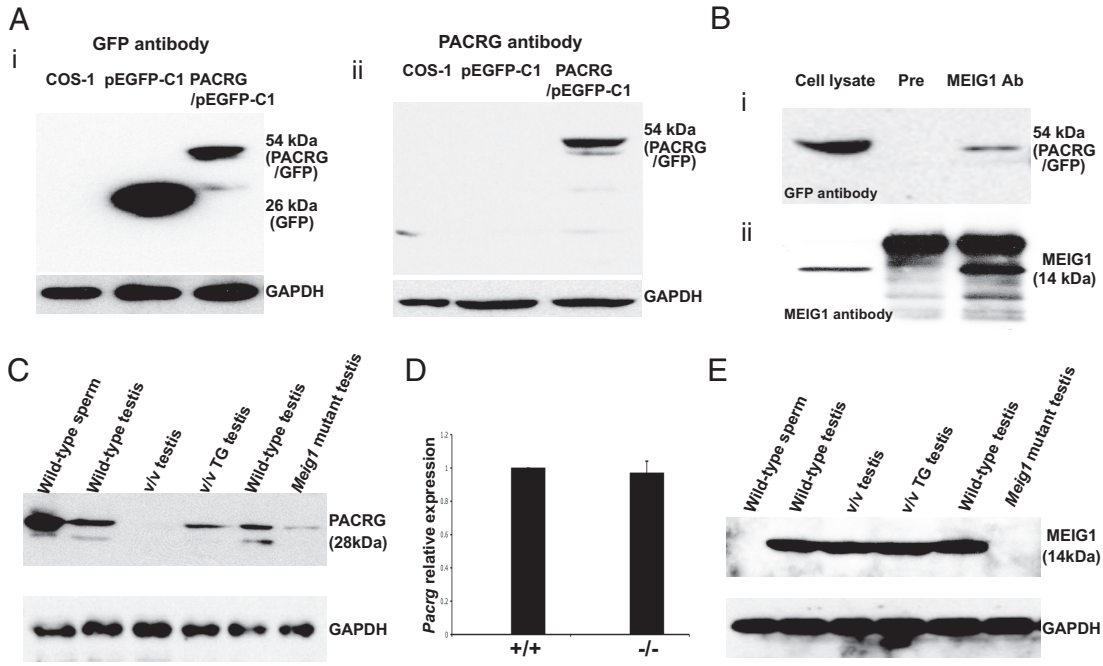

Fig. 4. MEIG1 associates with PACRG. (*A*) Expression of PACRG in COS-1 cells. COS-1 cells were transfected with the PACRG/pEGFP-C1 or empty pEGFP-C1 vector. Forty-eight hours after transfection, total cell lysates were prepared and Western blots were performed with an anti-GFP antibody (*i*) and an anti-PACRG antibody (*ii*). (*B*) Co-immunoprecipitation of MEIG1 and PACRG. COS-1 cells were co-transfected with PACRG/pEGFP-C1 and MEIG1/pTarget plasmids. Forty-eight hours after transfection, total cell lysates were pulled down with a preimmune serum or an anti-MEIG1 antibody. Western blots were conducted with an anti-GFP antibody (*i*) and an anti-MEIG1 antibody (*ii*). (*C*) Representative Western blot analysis of testicular PACRG protein expression in *Meig1* mutant mice. *v/v*: *quaking*^{viable} mutant mice; *v/v* TG: *Pacrg*-rescued *qk*^{v} mice. (*D*) Real-time PCR analysis of *Pacrg* mRNA expression in *Meig1* mutant mice. (*E*) Representative Western blot analysis of testicular MEIG1 protein expression in *Pacrg* mutant mice.

Discussion

The tissue distribution of the three *Meig1* tanscripts we identified is different. *Meig1_v1* is expressed in several tissues, including testis, lung, liver, and oocytes; it is the most abundant in the testis. *Meig1_v2* is expressed in almost all of the tissues tested, and the abundance is comparable in these tissues, suggesting that *Meig1_v2* is not a germ cell-specific transcript. *Meig1_v3* is only present in the testis, indicating that this is a testis-specific transcript.

The expression pattern of the three transcripts during the first wave of spermatogenesis is also different. *Meig1_v2* is stably expressed during the whole process of spermatogenesis, indicating it is a house-keeping isoform. This result contrasts with the results of previous studies, which suggested that 2a2 (*Meig1_v2*) was a germ cell-specific isoform (5–9). *Meig1_v1* and *Meig1_v3* are expressed from d20 and d12 after birth, respectively, indicating that that they are late-meiosis and postmeiosis-expressed isoforms, suggesting a special role at this stage. The presence of multiple *Meig1* transcripts in vivo suggests that the protein might have multiple functions depending upon cell type and timing of expression.

The phenotype of the *Meig1*-deficient mice generated using CMV-Cre excision was surprising, since previous studies suggested that MEIG1 might play a role in meiosis (5–9). However, we found that spermatocytes completed meiosis and spermatogenesis was arrested in the elongation and condensation stage, revealing that the MEIG1 is not necessary for meiosis, but is required for the completion of spermiogenesis.

With the exception of male infertility, no other phenotype related to immotile cilia syndrome was observed (15, 16), and the major feature of infertility is failure of spermiogenesis rather than sperm motility. Thus, *MEIG1* is not a major candidate for immotile cilia syndrome.

To further investigate the mechanisms of MEIG1 in the regulation of spermatogenesis, a yeast two-hybrid screen was conducted, and PACRG was identified to be a major partner of MEIG1 in the testis. The *Pacrg* gene is co-regulated with the *Parkin* gene, a gene involved in Parkinson's disease, and it is a reverse strand gene located upstream of the *Parkin* gene (17). In the quaking mouse, there is a deletion of approximately 1.17 Mb of mouse chromosome 17, referred to as the *quaking*^{viable} (*qk*^{v}) deletion, including the entire promoter region, the first five coding exons of *Parkin*, and the complete coding sequence of *Pacrg*. The deletion results not only in a neurological phenotype, including a severe lack of myelin and the tremor of voluntary movements from which quaking mice get their name, but also in male infertility (18, 19), a phenotype that mirrors that of the *Meig1* mutant mice described here. A subsequent study demonstrated that the infertility phenotype of the chromosome 17 deletion is due to deletion of the *Pacrg* gene (20).

Although studies have linked PACRG to certain genetic diseases, such as parkinsonism (21, 22), leprosy (23, 24), and even cancer (25, 26), further investigation conclusively established its role in ciliogenesis. Proteomics and biochemical studies revealed that it is a component of *Chlamydomonas reinhardtii* centriole/basal bodies (27, 28). In *Trypanosoma brucei*, two PACRG proteins localize along the full length of the axoneme. Ablation of both proteins by RNA interference knockdown experiments produced slow growth and paralysis of the flagellum due to disorganized axoneme structure (29). Of particular interest, variation in the human *PACRG* promoter was demonstrated to be a risk factor associated with azoospermia (30). A recent study demonstrated that PACRG associates with tubulin and microtubules (31).

The similar phenotypes of *Meig1* and *Pacrg* mutant mice, the direct interaction of the MEIG1 and PACRG proteins, and the fact that PACRG protein is markedly reduced in MEIG1-deficient mice, suggests that the two proteins regulate spermiogenesis through a common mechanism, and MEIG1 may stabilize PACRG and/or serve as a co-factor for PACRG action. Notably, the impact of the absence of these two proteins is on formation of the sperm flagella and not more broadly on cilia, as might have been anticipated from the studies on *Chlamydomonas* and trypanosomes. The severe defects in sperm head shaping and flagella formation suggest a failure of intramanchette transport, which plays a key role in shaping the spermatid head, centrosome, and tail (32), and it has been shown that centrosome and associated microtubules play an essential during spermiogenesis (33–35). The manchette is a transient microtubular structure assembled concurrently with the elongation and condensation of the spermatid nucleus and growth of the centrosome-derived axoneme (36, 37). Several findings suggest that the manchette can sort structural proteins to the centrosome and the developing sperm tail through a mechanism of intramanchette transport (IMT) (32). In addition, IMT can also transport cargo proteins necessary for spermatid nuclear condensation (38). Disruption of manchette structure in *Meig1* deficient mice may impair the intramanchette transport system, resulting in the failure of spermatid head shaping and the formation of flagella. Indeed, our ultrastructural analysis of testis of MEIG1-deficient mice revealed that normal manchette structures were not present or were severely disrupted, whereas they were observed in wild-type testis. The defect in formation of normal flagella does not appear to be caused by a failure to produce components of the axoneme and fibrous sheath, since the expression of flagellar genes, including *Spag6*, *Spag16L*, *Spag17*, and *Akap4* was not affected in MEIG1-deficient mice (Fig. S7). Moreover, genes involved in the remodeling that forms the sperm head or that encode proteins that localize to the sperm head such as transition protein 2 (Tnp2), testis-specific histone H1 (Histone H1t) and *Spag16S* were not altered in *Meig1* mutant mice. However, we cannot rule out the possibility that the expression of other genes playing important roles in flagellar formation and remodeling of the sperm head are altered in the absence of MEIG1. This possibility must be entertained since MEIG1 has been reported to bind chromatin, and because MEIG1 is also present in somatic cells of the testis, where it might affect spermatogenesis indirectly via interactions in the supporting Sertoli cells and/or Leydig cells. In the same yeast two hybrid screen, a protein that is present in the Chromatoid body was identified seven times, a RNA splicing factor was also identified five time, suggesting that MEIG1 might, in addition, play a role in RNA processing, which is required for spermiogenesis (39, 40).

In summary, we discovered that MEIG1, possibly through an interaction with PACRG, is essential for spermiogenesis, rather than its originally proposed role in meiosis. The profound sperm head and tail defects associated with the absence or disruption of normal manchettes, implicates MEIG1 as a critical gene for manchette structure and function and the control of spermiogenesis.

Methods

Rapid Amplification of cDNA Ends (RACE). 5′- and 3′- RACE were carried out to define the 5′- and 3′-untranslated region sequence of the mouse *Meig1* using mouse testis poly (A)$^{+}$ RNA and the Marathon cDNA amplification kit (Clontech) according to the manufacturer's instructions.

Generation of an Anti-MEIG1 Antibody. A cDNA encoding full-length MEIG1 was inserted into pET28a vector (Novagen). The resulting fusion protein was induced and subsequently purified as reported previously (41). The purified recombinant protein was used to generate polyclonal antisera in rabbits by a commercial organization (Rockland).

Targeted Disruption of *Meig1*. The 1.1-kb deletion region (exon 1 and flanking region) was amplified by PCR, and *Bam*HI and *LoxP* sites were added to the left end and a *Not*I site to the right end. The PCR product was digested with *Bam*HI/*Not*I, and cloned into the pBluescript plasmid (this construct was named M2/pBlue). A 5-kb left arm (red line in Fig. S3*A*) was amplified and cloned into *Cla*I/*Bam*H I sites of M2/pBlue to create M1, 2/pBlue construct. The 3-kb right arm (green line) was amplified by PCR and *Kpn*I sites were included on both ends. The PCR product was cloned into *Kpn*I site of the plasmid backbone for the knockout construct pND1(M3/pND1). The M1, 2/pBlue plasmid was digested with *Cla*I/*Not*I and cloned into M3/pND1 to finish the final construct. The resulting targeting construct was linearized by *Cla*I digestion at the plasmid/gene insert junction and

transfected into an XY ES line (TL) by electroporation. Positive ES cells were screened by PCR (primer sequences as shown in Table S1) and Southern blotting. Two positive ES cell clones were injected to generate chimeric mice.

Southern Blot Analysis. Fifteen micrograms of DNA from ES cells was digested with *Bam*HI and separated by 0.8% agarose gel electrophoresis. The DNA was transferred to nylon membranes and probed with a *Meig1* gene-specific probe upstream of the homologous recombination region.

Northern Blot Analysis. Northern blots containing total testicular RNA (30 μg per lane) were probed with a full-length coding region of mouse *Meig1* cDNA or other cDNAs for genes involved in sperm function.

Western Blot Analysis. An equal amount of indicated protein (50 μg per lane) was subjected to Western blot analysis by using indicated antibodies.

Histology and Transmission Electron Microscopy. Testes were prepared for light and electron microscopy by using standard methods (42).

Flow Cytometry. Fresh isolated mixed germ cells were washed twice in PBS and stained with a solution containing 50 μg/mL propidium iodide, 7k U/mL RNase B, and 0.1% Triton X-100 in Na Citrate (3.8 mM) at room temperature for 20 min. The stained cells were analyzed by using a FACScan flow cytometer.

Real-Time PCR. Total RNA was isolated from whole testes using TRIzol reagent (Invitrogen). RT and QPCR were carried out as previously described (43). The relative abundance of the targets were divided by the relative abundance of 18S rRNA in each sample to generate a normalized abundance for each transcript in each sample.

Yeast Two-Hybrid Screen. A pretransformed mouse testis cDNA library (Clontech) was screened with the full-length *Meig1* coding region as bait following the protocol provided in the kit.

Expression Vector Constructs. cDNAs containing the full length *Meig1* and *Pacrg*-coding sequences were generated by RT-PCR. After sequencing, *Meig1* cDNA was cloned into the *Bam*H1/*Xho*I site of the pTarget vector, *Pacrg* cDNA was cloned into cloned into the *Eco*RI/*Bam*HI sites of the pEGFP-C_1 vector, creating Meig1/pTarget and Pacrg/pEGFP-C_1 plasmids.

Co-immunoprecipitation. COS-1 cells were transfected with Meig1/pTarget and Pacrg/pEGFP-C1 plasmids. Forty-eight hours later, the cells were harvested into immunoprecipitation buffer (150 mM NaCl/50 mM Tris·HCl, pH 8.0/5 mM EDTA/1% Triton X-100/1 mM PMSF/proteinase inhibitor mixture), and the lysates were passed through a 20-gauge needle. After centrifugation at 11,600 $\times$ *g* for 5 min, the supernatants were precleared with protein A beads at 4 °C for 30 min. The supernatants were then incubated with preimmune serum (negative control) or an anti-MEIG1 polyclonal antibody at 4 °C for 2 h, and protein A beads were added with a further incubation at 4 °C overnight. The beads were washed with immunoprecipitation buffer three or four times, and loading buffer was then added to the beads, which were boiled at 100 °C for 10 min; the samples were then processed for Western blotting with monoclonal anti-GFP antibody and anti-MEIG1 antibody. Co-immunoprecipitation was also performed using testicular extracts of wild-type mice with the same procedure as described above except that 1 mg testicular protein was incubated with anti-PACRG polyclonal antibody or preimmune rabbit serum, and Western blot was conducted using an anti-MEIG1 antibody.

ACKNOWLEDGMENTS. We thank Glenn L. Radice and Igor Kostetskii for their suggestions of making *Meig1* conditional knockout construct; Dr. Rita Shiang (Virginia Commonwealth University) for providing CMV-Cre transgenic mice; and Emily Jumet and Sonya Washington for assistance in photographing light microscopic histology preparations. This work was supported by National Institutes of Health Grants HD37416 (to J.F.S.), HD 045783 (to J.C.H.), CA115503 (to M.J.J.), and in part by the Intramural Research Program of the National Institutes of Health, National Institute of Environmental Health Sciences Grant ZO1-ES070076 (to E.M.E.) and National Institute of Child Health and Human Development F31 Predoctoral Fellowship IF3IHD0G2314-01 (to D.R.G.). Tissue processing and staining were performed in Histology Core Facility of Virginia Commonwealth University. Transmission electron microscopy was performed in the Imaging Core of Virginia Commonwealth University (5P30NS047463).

1. Eddy EM (2002) Male germ cell gene expression. *Recent Prog Horm Res* 57:103–128.
2. Fawcett DW (1975) The mammalian spermatozoon. *Dev Biol* 44:394–436.
3. Tanaka H, Baba T (2005) Gene expression in spermiogenesis. *Cell Mol Life Sci* 62:344–354.
4. Krausz C, Sassone-Corsi P (2005) Genetic control of spermiogenesis: Insights from the CREM gene and implications for human infertility. *Reprod Biomed Online* 10:64–71.
5. Don J, Wolgemuth, DJ (1992) Identification and characterization of the regulated pattern of expression of a novel mouse gene, meg1, during the meiotic cell cycle. *Cell Growth Differ* 3:495–505.
6. Don J, Winer MA, Wolgemuth DJ (1994) Developmentally regulated expression during gametogenesis of the murine gene meg1 suggests a role in meiosis. *Mol Reprod Dev* 38:16–23.
7. Ever L, Steiner R, Shalom S, Don J (1999) Two alternatively spliced Meig1 messenger RNA species are differentially expressed in the somatic and in the germ-cell compartments of the testis. *Cell Growth Differ* 10:19–26.
8. Chen-Moses A, Malkov M, Shalom S, Ever L, Don J (1997) A switch in the phosphorylation state of the dimeric form of the Meg1 protein correlates with progression through meiosis in the mouse. *Cell Growth Differ* 8:711–719.
9. Steiner R, Ever L, Don J (1999) MEIG1 localizes to the nucleus and binds to meiotic chromosomes of spermatocytes as they initiate meiosis. *Dev Biol* 216:635–645.
10. Bouma GJ, Affourtit JP, Bult CJ, Eicher EM (2007) Transcriptional profile of mouse pre-granulosa and Sertoli cells isolated from early-differentiated fetal gonads. *Gene Expr Patterns* 7:113–123.
11. Tabuchi Y, Takasaki I, Kondo T (2006) Identification of genetic networks involved in the cell injury accompanying endoplasmic reticulum stress induced by bisphenol A in testicular Sertoli cells. *Biochem Biophys Res Commun* 345:1044–1050.
12. Zhang Z, et al. (2004) Haploinsufficiency for the murine orthologue of Chlamydomonas PF20 disrupts spermatogenesis. *Proc Natl Acad Sci USA* 101:12946–12951.
13. Wang G, Zhang J, Moskophidis D, Mivechi NF (2003) Targeted disruption of the heat shock transcription factor (hsf)-2 gene results in increased embryonic lethality, neuronal defects, and reduced spermatogenesis. *Genesis* 36:48–61.
14. McClintock TS, Glasser CE, Bose SC, Bergman DA (2008) Tissue expression patterns identify mouse cilia genes. *Physiol Genomics* 32:198–206.
15. Afzelius BA (1981) Genetical and ultrastructural aspects of the immotile-cilia syndrome. *Am J Hum Genet* 33:852–864.
16. Baccetti B, Burrini AG, Pallini V (1980) Spermatozoa and cilia lacking axoneme in an infertile man. *Andrologia* 12:525–532.
17. West AB, Lockhart PJ, O'Farell C, Farrer MJ (2003) Identification of a novel gene linked to parkin via a bi-directional promoter. *J Mol Biol* 326:11–19.
18. Bennett WI, Gall AM, Southard JL, Sidman RL (1971) Abnormal spermiogenesis in quaking, a myelin-deficient mutant mouse. *Biol Reprod* 5:30–58.
19. Lockhart PJ, O'Farrell CA, Farrer MJ (2004) It's a double knock-out! The quaking mouse is a spontaneous deletion of parkin and parkin co-regulated gene (PACRG). *Mov Disord* 19:101–104.
20. Lorenzetti D, Bishop CE, Justice MJ (2004) Deletion of the Parkin coregulated gene causes male sterility in the quaking (viable) mouse mutant. *Proc Natl Acad Sci USA* 101:8402–8407.
21. Lesage S, et al. (2007) Deletion of the parkin and PACRG gene promoter in early-onset parkinsonism. *Hum Mutat* 28:27–32.
22. Deng H, et al. (2005) Genetic analysis of parkin co-regulated gene (PACRG) in patients with early-onset parkinsonism. *Neurosci Lett* 382:297–299.
23. Malhotra D, et al. (2006) Association study of major risk single nucleotide polymorphisms in the common regulatory region of PARK2 and PACRG genes with leprosy in an Indian population. *Eur J Hum Genet* 14:438–442.
24. Alter A, Alcaïs A, Abel L, Schurr E (2008) Leprosy as a genetic model for susceptibility to common infectious diseases. *Hum Genet* 123:227–235.
25. Mulholland PJ, et al. (2006) Genomic profiling identifies discrete deletions associated with translocations in glioblastoma multiforme. *Cell Cycle* 5:783–791.
26. Toma MI, et al. (2008) Loss of heterozygosity and copy number abnormality in clear cell renal cell carcinoma discovered by high-density affymetrix 10K single nucleotide polymorphism mapping array. *Neoplasia* 10:634–642.
27. Keller LC, et al. (2005) Proteomic analysis of isolated chlamydomonas centrioles reveals orthologs of ciliary-disease genes. *Curr Biol* 15:1090–1098.
28. Ikeda K, Ikeda T, Morikawa K, Kamiya R (2007) Axonemal localization of Chlamydomonas PACRG, a homologue of the human Parkin-coregulated gene product. *Cell Motil Cytoskeleton* 64:814–821.
29. Dawe HR, Farr H, Portman N, Shaw MK, Gull K (2005) The Parkin co-regulated gene product, PACRG, is an evolutionarily conserved axonemal protein that functions in outer-doublet microtubule morphogenesis. *J Cell Sci* 118:5421–5430.
30. Wilson GR, et al. (2009) Molecular analysis of the Parkin co-regulated gene and association with male infertility. *Fertil Steril* Mar 5. [Epub ahead of print].
31. Ikeda T (2008) Parkin-co-regulated gene (PACRG) product interacts with tubulin and microtubules. *FEBS Lett* 582:1413–1418.
32. Kierszenbaum AL (2002) Intramanchette transport (IMT): Managing the making of the spermatid head, centrosome, and tail. *Mol Reprod Dev* 63:1–4.
33. Manandhar G, Simerly C, Salisbury JL, Schatten G (1999) Centriole and centrin degeneration during mouse spermiogenesis. *Cell Motil Cytoskeleton* 43:137–144.
34. Manandhar G, Sutovsky P, Joshi H-C, Stearns T, Schatten G (1998) Centrosome reduction during mouse spermiogenesis. *Dev Biol* 203:424–434.
35. Schatten G (1994) The centrosome and its mode of inheritance: The reduction of the centrosome during gametogenesis and its restoration during fertilization. *Dev Biol* 165:299–335.
36. Clermont Y, Oko R, Hermo L (1993) Cell Biology of Mammalian Spermatogenesis. In *Cell and Molecular Biology of the Testis*, eds Desjardins C, Ewing LL. (Oxford University Press, New York), pp 332–376.
37. Meistrich ML (1993) Nuclear morphogenesis during spermiogenesis. In *Molecular Biology of the Male Reproductive System*, ed de Kretser D. (Academic, New York), pp 67–97.
38. Kierszenbaum AL, Rivkin E, Tres LL (2007) Molecular biology of sperm head shaping. *Soc Reprod Fertil Suppl* 65:33–43.
39. Vasileva A, Tiedau D, Firooznia A, Müller-Reichert T, Jessberger R (2009) Tdrd6 is required for spermiogenesis, chromatoid body architecture, and regulation of miRNA expression. *Curr Biol* 19:630–639.
40. Zhang Z, et al. (2002) A sperm- associated WD repeat protein orthologous to Chlamydomonas PF20 associates with Spag6, the mammalian orthologue of Chlamydomonas PF16. *Mol Cell Biol* 22:7993–8004.
41. Paronetto MP, et al. (2009) Sam68 regulates translation of target mRNAs in male germ cells, necessary for mouse spermatogenesis. *J Cell Biol* 85:235–249.
42. Sapiro R, et al. (2002) Male infertility, impaired sperm motility, and hydrocephalus in mice deficient in sperm-associated antigen 6. *Mol Cell Biol* 22:6298–6305.
43. Horowitz E, et al. (2005) Patterns of expression of sperm flagellar genes: Early expression of genes encoding axonemal proteins during the spermatogenic cycle and shared features of promoters of genes encoding central apparatus proteins. *Mol Hum Reprod* 11:307–317.